

# Post-AGB Stars with Circumbinary Discs

Tyl Dermine<sup>1,2</sup>, Robert G. Izzard<sup>1</sup>, Alain Jorissen<sup>2</sup>, and Hans Van Winckel<sup>3</sup>

<sup>1</sup> Argelander-institut für Astronomie, University of Bonn, Auf dem Hügel 71, D-53121 Bonn, Germany

<sup>2</sup> Institut d'Astronomie et d'Astrophysique, Université Libre de Bruxelles, Belgium

<sup>3</sup> Instituut voor Sterrenkunde, K.U.Leuven, Belgium

## Abstract

Circumbinary discs are commonly observed around post-asymptotic giant branch (AGB) systems and are known to play an important role in their evolution. Several studies have pointed out that a circumbinary disc interacts through resonances with the central binary and leads to angular momentum transfer from the central binary orbit to the disc. This interaction may be responsible for a substantial increase in the binary eccentricity. We investigate whether this disc eccentricity-pumping mechanism can be responsible for the high eccentricities commonly found in post-AGB binary systems.

**Key words.** Stars: binaries – Stars: post-AGB – Stars: chemically peculiar – Galaxy: stellar content

## 1. Introduction

Post-AGB stars just left the AGB phase and evolve rapidly to hotter effective temperatures at constant luminosity, but they are not yet hot enough to ionise circumstellar material ejected during the AGB phase. Some post-AGB stars also show a near-infrared emission due to thermal radiation of hot circumstellar dust. The colour temperature of the dust is a good indication that there must be circumstellar dust close to the star and this SED characteristic is always related to binarity (Van Winckel et al. 2009, and references therein). The extremely narrow CO emission lines (a few  $\text{km s}^{-1}$  width, e.g. Jura et al. 1995), the presence of large (sub-micron) grains (Gielen et al. 2011) and the detection of Oxygen-rich crystalline silicates (Waters et al. 1998) are distinct characteristics best explained by the long-term processing of dust in a stable circumbinary (CB) disc.

However, a key problem still remains regarding the inability of population-synthesis models to reproduce the observed large eccentricities of post-AGB stars, similarly observed in barium stars (Pols et al. 2003; Izzard et al. 2010). In the previous evolutionary phase (i.e. the AGB), the very large stellar radii lead to efficient circularisation of the binary orbit by tides (Zahn 1977). Systems too close to accommodate an AGB star undergo Roche-lobe-overflow (RLOF) mass transfer, in most cases in an unstable regime which leads the system into a common envelope (CE). Due to friction between the stellar cores and the CE, the envelope may be ejected, and the orbit shrunk and circularised. Post-AGB binaries with orbital periods shorter than 1,000 d are expected to be circular whereas observations reveal instead systems with periods from about  $10^2$  d to 3,000 d, often in eccentric orbits. A mechanism that increases the binary eccentricity is therefore required.

If tides are as efficient as predicted (Zahn 1977), a mechanism to increase the eccentricity must take place during the AGB or post-AGB evolution. Different mechanisms have been investigated such as enhanced mass-transfer at periastron (i.e. differential mass loss dur-

ing an orbital period; Soker 2000), eccentricity pumping induced by a wind-RLOF hybrid mass transfer (Bonačić Marinović et al. 2008) and a kick to the newly-born white dwarf (Izzard et al. 2010).

In this paper we investigate the possibility that CB discs cause the large eccentricities observed in some post-AGB systems. The current knowledge of CB discs is summarised in Section 2. In Section 3 we present our results and compare them to observed post-AGB periods and eccentricities. Section 4 discusses successes and potential problems of our model. Conclusions are drawn in Section 5.

## 2. Circumbinary discs

In this section we enumerate the classes of stars known or suspected to be binaries that possess dust discs.

### 2.1. Observed disc properties

Dust discs are observed in very different classes of stars known to be binaries (Chesneau 2011). Stable discs are observed around most known post-AGB binaries (Van Winckel 2003; de Ruyter et al. 2006; Van Winckel et al. 2006). They are increasingly being identified around the central stars of planetary nebulae, e.g. NGC 2346 (Costero et al. 1986). Other evidence exists such as eclipses from dust discs (in NGC 2346, CPD-56°8032 and M2-29, Hajduk et al. 2008; Gesicki et al. 2010). Some symbiotic stars (Angeloni et al. 2007), hydrogen-deficient binary (Netolický et al. 2009) and young stellar objects (Deroo et al. 2007a) are also known to possess long-lived CB discs. Around some silicate J-type stars, the disc is resolved (Deroo et al. 2007b). Some AGB stars (e.g. X Her ; Kahane & Jura 1996) have a very slowly expanding wind (a few  $\text{km s}^{-1}$ ), however none is a confirmed binary system. Keplerian discs are also observed in B[e] stars (Meilland et al. 2007); but only few B[e] stars are confirmed binaries and it remains unclear whether the B[e] behavior is

related to binarity (Lamers et al. 1998). Finally, discs have been discovered around white dwarfs (e.g. Gänsicke et al. 2006). Surveys for such discs around the oldest white dwarfs have been unsuccessful (Kilic et al. 2009), but around 15% of local white dwarfs show metal-rich material in their photosphere, indicative of accretion from a residual dust reservoir (Sion et al. 2009), although this reservoir may not necessarily originate from binary interaction.

The variety of classes of objects that host CB discs and the wide range of orbital periods of the central stars (from 115.9 d for SAO 173329 - van Winckel et al. 2000 - to 2597 d for U Mon; Pollard & Cottrell 1995) show that they are very common around binary systems and easily formed in *late-type mass-transfer* systems. The structure of discs surrounding young stellar objects and post-AGB stars is somewhat similar (de Ruyter et al. 2006), which is rather remarkable because of their (possibly) very different formation mechanism.

The stable nature of the dust disc in post-AGB systems can be inferred from the observation that none of them shows evidence for a current dusty mass-loss while the dust excess starts near dust-sublimation radius; the near-IR emitting material must be gravitationally bound in the system. In addition, post-AGB systems show depletion patterns, i.e. the gas in the disc is separated from the dust and subsequently reaccreted onto the star (Waters et al. 1992; Maas et al. 2005). This re-accretion process occurs more efficiently if circumstellar gas and dust are trapped in a stable disc (Van Winckel et al. 2006; de Ruyter et al. 2006; Gielen et al. 2008). Furthermore the presence of *near-IR* (from about 5 to 20  $\mu\text{m}$ ) excesses indicates that in all systems the circumstellar shell is not freely expanding but stored in a disc. The detection of cool (from about 100 to 150 K) Oxygen-rich *crystalline* silicate dust grains (Waters et al. 1998) as well as the presence of large (sub-micron) grains are other indications of the long-lived nature of these discs (e.g. Angeloni et al. 2007; Gielen et al. 2008). In some cases, Keplerian rotation is detected at least in the inner disc region (Bujarrabal et al. 2005).

## 2.2. Formation

The formation of CB discs and their impact on the central star is not well understood. Most likely, CB discs in post-AGB stars remain from CE ejection or form during mass-transfer events in a binary system. The former case is supported by population synthesis models which show that most post-AGB systems that possess a CB disc are post CE systems. The possibility to form a CB disc from a fraction of the ejected CE has already been suggested from detailed CE models (Sandquist et al. 1998; Nordhaus & Blackman 2006; Kashi & Soker 2011). It turns out that the CE is not necessarily completely ejected, so some gas remains around the system. While CE evolution is expected to lead systems to orbital periods of hours to hundreds of days, no disc has been observed around systems with periods shorter than a hundred days.

On the other hand, many studies have investigated the possibility that matter flows through the second Lagrangian point  $L_2$  during RLOF (e.g. Podsiadlowski et al. 1992; Frankowski & Jorissen 2007; van Rensbergen et al. 2011), possibly because of radiation pressure which could reshape the Roche equipotentials by a reduction of the effective gravity of the mass-losing star (Schuerman

1972; Frankowski & Tylenda 2001; Dermine et al. 2009). Hydrodynamical simulations have shown that this can lead to the formation of a CB disc in a close binary system (Syrov et al. 2009). However, the disc may not be stable and may disappear as soon as the mass transfer stops. Two-dimensional hydrodynamical simulations show that, for a typical slow and massive wind from an AGB star, the flow pattern is similar to Roche lobe overflow, and that a small fraction of the mass transferred to the companion flows through  $L_2$  (de Val-Borro et al. 2009; Mohamed & Podsiadlowski 2010). The companion focuses the ejected material into the equatorial plane of the system (Theuns & Jorissen 1993; Theuns et al. 1996; Mastrodemos & Morris 1998). However, the possibility of forming a stable CB disc from a mass-losing giant star has not yet been confirmed by simulations.

## 2.3. Evolution

Surveys performed at wavelengths as long as 100  $\mu\text{m}$  show that none of the post-AGB systems with a disc is observed to be surrounded by an outflow remaining from the AGB phase (Gielen et al. 2011). This means that the observed post-AGBs have left the AGB phase long enough ago for the last ejecta of the AGB star to reach a distance at which the emission at 100  $\mu\text{m}$  cannot be detected. A lower limit of the disc lifetime can then be inferred. Using the code DUSTY (Ivezic & Elitzur 1997) for a post-AGB star with an effective temperature of 4,000 K, a luminosity of 5,000  $L_\odot$  and a wind composed only of silicate grains, we deduce a distance of about 0.4 pc. Assuming a typical wind velocity of 15  $\text{km s}^{-1}$ , this timescale is approximately  $2.5 \times 10^4$  yr.

It is known that the CB-disc mass decreases during post-AGB and PN phases because material flows away from the outer part of the disc and reaccretes on the central stars. Gesicki et al. (2010) pointed out the sharp decrease in CB-disc mass as the star ages. Finally, the discs observed around cooling white dwarfs have very low masses because all the gas was probably expelled and only the dust remains. An upper limit of the disc lifetime can then be estimated from the time since the mass transfer stopped, i.e. the end of the AGB phase, given by the timescale to cross the post-AGB and PN phases. While it has been estimated for single stars (of the order of 1,000 – 10,000 yr; Blöcker 1995), this timescale is very uncertain for binaries. In single stars, the post-AGB phase ends as soon as the thin envelope remaining from the AGB phase is entirely ejected. However if re-accretion occurs, e.g. from a CB disc, the envelope ejection could take much longer, possibly up to  $10^5$  yr. From the observed strongly depleted post-AGB stars in the LMC (Reyniers & van Winckel 2007; Gielen et al. 2009), we can infer a dilution of their envelopes by a factor of about 10. As the typical envelope mass is about  $10^{-3} M_\odot$  (Blöcker 1995),  $10^{-2} M_\odot$  must have been accreted from a CB disc. With a typical mass-loss rate of  $10^{-7} M_\odot \text{yr}^{-1}$ , the accreted mass therefore extends the post-AGB lifetime by about  $10^5$  yr.

The disc lifetime is determined by two competing mechanisms: (i) disc accretion (Hartmann et al. 1998), and (ii) photoevaporation of the surface layer of the gas disc due to far- and extreme-ultraviolet radiation from the central star (Hollenbach et al. 2000). For comparison, pre-main-sequence disc lifetimes are thought to be 5 – 10 Myr (Yasui et al. 2010).

Once the star is on the white-dwarf cooling track, any further dissipation is set by the Poynting-Robertson drag (Weidenschilling & Jackson 1993), with a time scale of the order of  $10^7$  yr. The disc may remain detectable for about  $10^8$  yr, long after any sign of the planetary nebula has disappeared.

#### 2.4. Resonant interactions

Goldreich & Tremaine (1979) and Artymowicz & Lubow (1994) describe the resonant and nonresonant interactions between a binary system and its CB disc using a linear perturbation theory and assuming (i) the disc is thin ( $0.01 < H/R < 0.1$ , where  $H$  and  $R$  are the thickness and the half angular momentum radius of the disc respectively) and (ii) the nonaxisymmetric potential perturbations are small around the average binary potential. The binary potential is expanded in a series as

$$\Phi(r, \theta, t) = \sum_{m,l} \phi_{m,l}(r) \exp [i m (\theta - (l/m)\Omega_b t)], \quad (1)$$

of which only the real part is relevant, and  $l$  and  $m$  are integers.  $\Omega_b$  is the orbital angular frequency which, in an inertial frame, is  $\Omega_b = \left(\frac{GM}{a^3}\right)^{1/2}$ , where  $a$  is the semi-major axis of the system, and  $M$  its total mass. The individual potential harmonics  $\phi_{m,l}(r)$  rotate uniformly with pattern speed

$$\Omega_p = (l/m)\Omega_b. \quad (2)$$

A resonance occurs in the disc when the pulsation  $\kappa$  of radial motion of a disc particle (on an epicyclic orbit with azimuthal pulsation  $\Omega$ ) is commensurate with the angular frequency ( $\Omega - \Omega_p$ ) in the frame rotating with component ( $l, m$ ) of the perturber,

$$m(\Omega - \Omega_p) = \pm \kappa, \quad (3)$$

where the positive/negative sign corresponds to the outer/inner Lindblad resonance (LR) respectively. A corotation resonance (CR) occurs when  $\Omega = \Omega_p$ . These resonant interactions result in the excitation of density waves located at radii

$$r_{\text{CR}} = (m/l)^{2/3} a, \quad (4)$$

and

$$r_{\text{LR}} = [(m \pm 1)/l]^{2/3} a. \quad (5)$$

Many studies have investigated whether these resonances increase the orbital eccentricity (Artymowicz et al. 1991; Artymowicz & Lubow 1994; Frankowski & Jorissen 2007). We apply the model of Lubow & Artymowicz (1996) for small and moderate eccentricities ( $e \lesssim 0.2$ ). This model is based on results of SPH simulations which show that for a disc in which the kinematic viscosity,  $\nu$ , is independent of the density, the torque is independent of resonance strength and width. The resonant torque can then be estimated from the rate of change of the disc angular momentum. The viscous torques within the disc balance the gravitational torque generated by resonances in the inner part of the disc and redistribute mass and angular momentum throughout the disc. The viscous torque is

$$\dot{J}_d = J_d/\tau = M_d \Omega_b \nu, \quad (6)$$

where the viscous timescale  $\tau = R^2/\nu = \alpha^{-1}(H/R)^{-2}\Omega^{-1}$  is of the order of  $10^5$  yr, and  $M_d$ ,  $\nu$  and  $\alpha$  are the mass,

kinematic viscosity and the viscosity parameter of the disc respectively. The viscosity parameter is typically  $\alpha \approx 0.1$ .

The variation of the orbital separation due to the resonant interaction between the binary and the CB disc is given by (Lubow & Artymowicz 1996)

$$\frac{\dot{a}}{a} = 2 \frac{\dot{J}_d \Omega_p}{J_{\text{orb}} \Omega_b} = -\frac{2l}{m} \frac{M_d}{\mu} \alpha \left(\frac{H}{R}\right)^2 \frac{a}{R} \Omega_b, \quad (7)$$

where  $J_{\text{orb}}$  is the orbital angular momentum and  $\mu$  is the reduced mass of the binary system. The increase of the eccentricity due to resonances can be given as a function of  $\dot{a}/a$  and depends on the binary eccentricity. At very small eccentricities ( $e \leq 0.1\alpha^{1/2}$ ), the resonances weakly drive the eccentricity so the inner radius of the CB disc is maintained by the  $m = l$  resonances that take place close to the binary at  $r/a \lesssim 1.7$ . The eccentricity pumping in that regime increases with  $e$  and is estimated (Lubow & Artymowicz 1996) to proceed as

$$\dot{e} = -\frac{50e}{\alpha} \frac{\dot{a}}{a}, \quad (8)$$

up to a maximum of  $\dot{e} = 5\alpha^{-1/2}\dot{a}/a$  at  $e \simeq 0.1\alpha^{1/2}$ . At larger eccentricities ( $0.1\alpha^{1/2} \lesssim e \lesssim 0.2$ ), the  $m = 2, l = 1$  resonance is the strongest contribution to the eccentricity driving and the disc is progressively pushed away as the binary eccentricity increases. In that regime, the eccentricity pumping decreases as  $1/e$ . The eccentricity growth diminishes as  $1/e$  until  $e \simeq 0.5 - 0.7$ , at which point resonances that damp the eccentricity begin to dominate (e.g. Rödiger et al. 2011). To include this effect, we assume the  $e$ -pumping to be inefficient ( $\dot{e} = 0$ ) for  $e \geq 0.7$  (note however that  $\dot{a}$  is not necessarily 0). The  $e$ -pumping efficiency for very small and moderate eccentricities (i.e. for  $e \lesssim 0.2$ ) is shown in Fig. 1 and is given by (see Lubow & Artymowicz 1996, 2000)

$$\dot{e} = \frac{2(1-e^2)}{e + \frac{\alpha}{100e}} \left(\frac{l}{m} - \frac{1}{\sqrt{1-e^2}}\right) \frac{\dot{a}}{a}. \quad (9)$$

The inner radius of the disc,  $r_{\text{in}}$ , is determined by the condition that the resonant torque, which tends to push the disc away, overcomes the viscous torque which acts to fill the inner region. Artymowicz & Lubow (1994) estimate from SPH simulations the disc inner radius at different binary eccentricities and for different Reynolds number of the disc gas,  $\mathcal{R} = (H/R)^{-2}\alpha^{-1}$  (see Fig. 3 of Artymowicz & Lubow 1994) which we fit with

$$r_{\text{in}}(e, \mathcal{R}) = 1.7 + \frac{3}{8} \log(\mathcal{R}\sqrt{e}) \text{ AU}. \quad (10)$$

Finally, the variation of the orbital angular momentum in the centre-of-mass frame is given by

$$\dot{J}_{\text{orb}} = J_{\text{orb}} \frac{\dot{a}}{2a} - J_{\text{orb}} \frac{e\dot{e}}{(1-e^2)}. \quad (11)$$

Our model is in reasonable (within a factor two) agreement with the SPH results of Artymowicz et al. (1991), who give  $\dot{a}/a \simeq -4.3 \times 10^{-4} \Omega_b M_d/M_b$  and  $\dot{e} \simeq 1.9 \times 10^{-3} \Omega_b M_d/M_b$  at  $e = 0.1$ , for  $\mu = 0.3$ ,  $\alpha = 0.1$ ,  $\mathcal{R} = 10^3$ , with a CB disc extending from  $r = 1.7a$  to  $r = 6a$ , with a surface density distribution  $\sigma \propto r^{-1}$ . Our model gives  $\dot{a}/a \simeq -2.8 \times 10^{-4} \Omega_b M_d/M_b$  and  $\dot{e} \simeq 2.5 \times 10^{-3} \Omega_b M_d/M_b$ .

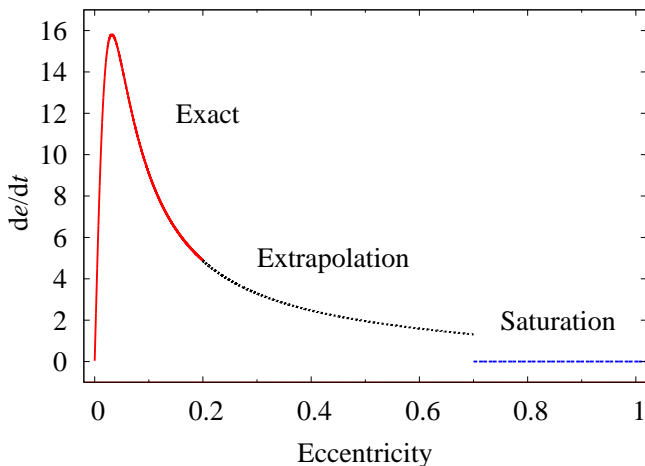


**Figure 1.**  $de/dt$  in units of  $d \ln a/dt$  as a function of  $e$  (Eq. 9) based on a model for very low and moderate eccentricities (Lubow & Artymowicz 1996, 2000), for a circumbinary disc with a viscosity parameter  $\alpha = 0.1$ . The curve is divided in three regions. For eccentricities from 0 to 0.2, our model is strictly valid (red solid curve). For eccentricities from 0.2 to 0.7, the model is extrapolated outside its validity range according to an efficiency decreasing as  $1/e$  (black dotted curve). At higher eccentricities,  $de/dt = 0$  to account for the saturation behavior (blue dashed curve).

### 2.5. Eccentricity gap

Interestingly, pre-MS and MS systems lack nearly circular orbits at long periods (called the *eccentricity gap*; see Mathieu 1992, 1994), whereas short-period systems are circularised by tides. Although the eccentricity distribution of pre-MS and MS systems is likely the result of numerous processes such as binary formation, stellar encounters and tides, interaction with a CB disc certainly occurs as well. Discs commonly observed in pre-MS systems are similar to those observed around post-AGB stars (de Ruyter et al. 2006), with masses from  $0.004$  to  $0.3 M_{\odot}$ . Artymowicz et al. (1991), Artymowicz & Lubow (1994), Mathieu et al. (1995) and Lubow & Artymowicz (1996) suggest that they pump the binary eccentricity, which explains the eccentricity gap. Note however the surprising exception of GW Orionis, a system still embedded in a disc of  $M_d \approx 0.3 M_{\odot}$ , with a period of 242 d and an unexpected low eccentricity of  $e \approx 0.04 \pm 0.06$  (Mathieu et al. 1991). Following the evolution of pre-MS with disc-binary interaction is however not the scope of this paper.

Note that an eccentricity gap seems also present in post-AGB binaries (see Fig. 3) with periods longer than  $10^3$  d, in which tides are inefficient.

## 3. Modelling post-AGB binaries with circumbinary discs

We introduce the CB-disc properties and apply our model of Section 2.4 to derive the evolution of post-AGB systems in the period-eccentricity plane.

### 3.1. Circumbinary disc model

The post-AGB disc properties can be derived from spectral-energy-distribution (SED) modelling in the near-

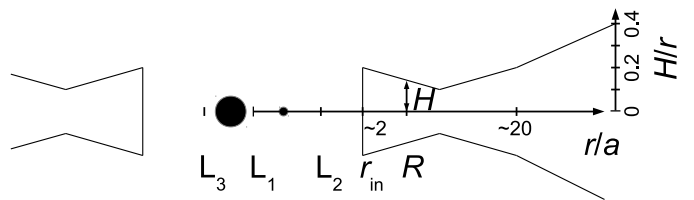


**Figure 2.** Disc geometry as described in Dullemond et al. (2001).  $L_1$ ,  $L_2$  and  $L_3$  are the Lagrangian points, where forces cancel out.  $r_{in}$ ,  $R$  and  $H$  are the inner radius, the half angular-momentum radius and the thickness of the disc, respectively. The given radii are indicative.

| Parameter           | Range                    | Adopted           |
|---------------------|--------------------------|-------------------|
| $M_d/M_{\odot}$     | $10^{-4} - 10^{-2}$      | $10^{-2}$         |
| $t_d/\text{yr}$     | $2.5 \times 10^4 - 10^5$ | $2.5 \times 10^4$ |
| $\alpha$            | 0.01 – 0.1               | 0.1               |
| $H/R$               | 0.1 – 0.2                | 0.1               |
| $r_{in}$            |                          | Eq. 10            |
| $r_{out}/\text{AU}$ | 100 – 2,000              | 500               |
| $\mu/M_{\odot}$     |                          | 0.3               |

**Table 1.** Possible range and adopted values of the parameters, where  $M_d$ ,  $t_d$ ,  $\alpha$ ,  $H/R$ ,  $r_{in}$  and  $r_{out}$  are the mass, the lifetime, the viscosity parameter, the thickness, the inner radius and the outer radius of the circumbinary disc, respectively (see also Fig. 2).  $\mu$  is the reduced mass of the binary. See Section 3.1 for more details.

IR. Observed disc masses range from about  $10^{-4}$  to  $10^{-2} M_{\odot}$  (Gielen et al. 2007). The relative thickness near the inner edge is  $H/R = 0.1 - 0.25$  (Dullemond et al. 2001). However, as our model is only valid for thin discs, we assume  $H/R = 0.1$ .

The inferred location of the inner disc edge mainly depends on the opacity of the grains which in turn is related to their chemistry and size distribution. Metallic iron has no spectral feature but a large opacity so, depending on the adopted abundance of iron, the SED can be fitted with different inner radii ranging from about 2 to 10 AU. These values are in good agreement with our predicted inner radius (Eq. 10) assuming typical separations of post-AGB systems from about 0.5 to 5 AU. The outer radius ranges from about 100 to a few thousands AU (de Ruyter et al. 2006) and is taken to be  $r_{out} = 500$  AU. The surface density distribution decreases with distance from the centre of the disc,  $\sigma(r) \propto r^{\delta}$ , with  $-2 \lesssim \delta \lesssim -1$  (de Ruyter et al. 2006). In our model, we choose  $\sigma(r) \propto r^{-2}$  such that the half-angular-momentum radius is  $R = \sqrt{r_{in} r_{out}}$ .

Since when  $e = 0$  the pumping of the eccentricity is ineffective ( $\dot{e} = 0$ ), we assume that perturbations of the orbit, e.g. due to the CB disc or to stellar pulsation lead to a minimum eccentricity of  $10^{-3}$ .

### 3.2. Post-AGB evolution in the $e - \log P$ plane with CB disc interaction

In Fig. 3 we show four evolutionary tracks in the  $e - \log P$  plane of post-AGB systems with initial periods of 100 d,

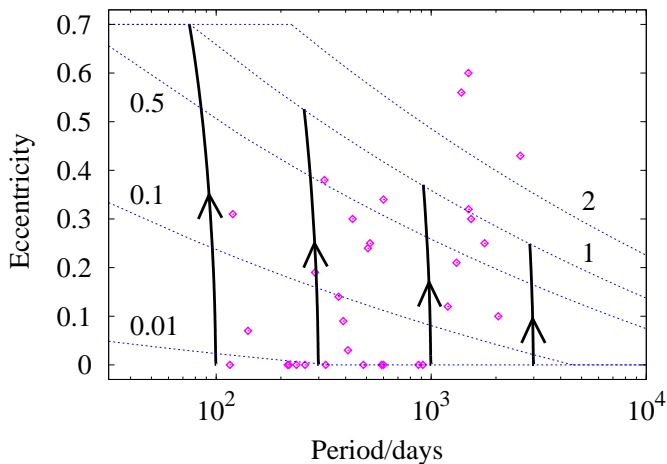


**Figure 3.** Evolutionary tracks during the post-AGB phase (black lines) in the  $e - \log P$  plane including the interaction with a circumbinary disc as described by Eqs. 7 and 9 (see also Fig. 1) with the adopted circumbinary-disc properties of Table 1. The  $\diamond$  symbols are observed post-AGB systems. The blue dashed lines show the final eccentricity corresponding to eccentricity-pumping as given by Eq. 9, modulated by the labelled values (1 corresponds to the adopted parameters). The timescale needed to pump the eccentricity can be estimated from Eq. 12.

300 d, 1,000 d and 3,000 d, which interact with a CB disc with properties as given in column 3 of Table 1. The binary systems are characterised by a reduced mass  $\mu = 0.3 M_{\odot}$ . Their orbits are initially circular because tides are very efficient during the AGB phase and circularise all systems with  $P \lesssim 2,000$  d. Longer-period systems can remain eccentric at the start of the post-AGB phase. The blue dashed lines indicate the final binary eccentricity due to eccentricity-pumping as given by Eqs. 7 and 9 for different disc properties. Each line corresponds to pumping modulated by the labelled value. For example, the line labelled 0.5 corresponds to the case where  $\dot{e}$  is decreased by a factor 2 compared to our adopted case (labelled 1).

The mass and lifetime of the disc are  $M_d = 10^{-2} M_{\odot}$  and  $t_d = 2.5 \times 10^4$  yr, respectively, which correspond to the highest mass observed and to a lower limit of the disc lifetime. As expected from Eqs. 7 and 9, the  $e$ -pumping decreases with increasing period because of the dependence of  $\dot{e}$  on the orbital period, i.e.  $\dot{e} \propto a \Omega_b \propto P^{-1/3}$ . However, this trend is not observed among the post-AGB stars (see discussion in Section 4.2). Nevertheless, our simulations can reproduce the observed eccentricities of all post-AGB systems, except for the three systems with  $P > 10^3$  d and  $e > 0.4$ . Moreover, all the systems are not equally evolved on the post-AGB phase, so some systems may have interacted longer with their CB disc leading to a more eccentric orbit. When extending the disc lifetime to  $10^5$  yr, its expected maximum lifetime, our model predicts systems with  $e = 0.7$  at  $P \sim 10^3$  d (see Eq. 12).

## 4. Discussion

### 4.1. Model uncertainties

The time to pump the binary eccentricity from 0 to  $e_f$  is given by

$$t(e_f) = 2 \times 10^5 e_f^2 \frac{\mu}{0.3} \frac{10^{-2} M_{\odot}}{M_d} \frac{0.1}{\alpha} \left( \frac{0.1}{H/R} \right)^2 \left( \frac{P}{1000 \text{ d}} \right)^{2/3} \sqrt{\frac{r_{\text{out}}}{500 \text{ AU}}} \text{ yr.} \quad (12)$$

Regarding the possible range of the disc parameters (i.e.  $M_d$ ,  $t_d$ ,  $\alpha$ ,  $H/R$  and  $r_{\text{out}}$ ) given in Table 1, the eccentricity-pumping efficiency can be increased by a factor 36 or decreased by a factor 2000 compared to the adopted values. Fig. 3 shows that for an efficiency decreased by a factor more than 100, the CB disc has a no significant effect on the binary eccentricity any more.

### 4.2. Discussion

Our model is able to reproduce most orbits of post-AGB binaries except for the three systems at  $P > 10^3$  d and  $e > 0.4$  (Fig. 3). Extending the disc lifetime to  $10^5$  yr, the expected upper limit, gives enough time for the CB disc to increase the system eccentricity to the observed value. However, systems with periods longer than about 2,000 d are not efficiently circularised during the AGB phase, so they can start the post-AGB phase in an eccentric orbit. Moreover, as the CB disc is formed during the AGB phase, eccentricity pumping takes place before the post-AGB phase. This leads to an underestimation of the binary eccentricity at  $P \gtrsim 2,000$  d. At shorter periods, binary systems enter a CE which circularises the orbit before the system starts its evolution on the post-AGB phase.

There is an important discrepancy between the expected and observed distributions of post-AGB systems in the period-eccentricity plane. Our model predicts systems with eccentricities that decreases with increasing periods while the observed distribution shows the opposite. As discussed before, this discrepancy may partly be explained by an underestimation in our model of the eccentricity at long orbital periods. A hypothesis to explain this discrepancy is that the properties of the disc and the binary are correlated in such a way that  $e$ -pumping is more efficient in longer-period systems. It would be a surprise if discs that form through wind mass-transfer or remaining from CE ejection are similar. However, our understanding of disc formation is poor, so no *a priori* correlation can be suggested. None of the observed disc properties are correlated with the binary properties. Nonetheless, it is surprising that no post-AGB stars with a disc are observed in systems with orbital periods shorter than 100 d. From binary evolutionary models, such systems are predicted to exist as post-CE systems and are expected to have periods from a few hours to hundreds of days. As none are observed, CB discs may be very short-lived or unstable at periods shorter than about 100 d.

In our model we do not consider accretion of matter onto the central stars or outflow from the disc. While the effects of such re-accretion are observed in some post-AGB stars (Waters et al. 1992), our model disc mass is assumed constant for simplicity. However, as discussed in Section 2.3, the post-AGB systems are observed at least  $10^4$  yr after they left the AGB phase. The inferred disc masses thus represent a lower limit of their initial masses. Note that the most important effect of re-accretion is to slow down the evolution along the post-AGB phase. It then takes longer for the central star to become hot enough to efficiently evaporate

orate the disc gas due to ultraviolet radiation compared to single star evolution where no accretion takes place.

The conclusions reached in this paper not only concern post-AGB systems, but a variety of classes of post-mass transfer systems such as barium stars, S stars, subgiant CH and CEMP binaries, which we observe long after mass transfer finished. If CB discs play an important role in the evolution of post-AGB systems they are also relevant for these classes of stars. Their similar periods and eccentricities to post-AGB stars support an identical eccentricity-pumping mechanism. We are currently working on population synthesis models including the formation and interaction with a CB disc, which attempts at explaining the orbital properties of all these systems (Dermine et al. 2012, in preparation).

## 5. Conclusions

Our circumbinary-disc model describes the resonant interaction between a disc and its central binary with which we account for the large eccentricities observed among post-AGB stars. Stable dust discs are detected in a large fraction of post-AGB stars and are known to be closely related to binarity. Circumbinary discs strongly alter the evolution of the binary system because of resonant interactions and reaccretion from the circumbinary disc. Resonant interactions with a circumbinary disc transfer angular momentum from the binary orbit to the disc and increases the binary eccentricity. We use the model described by Lubow & Artymowicz (1996) with the disc properties derived from the observed SED of post-AGB stars. Reaccretion of gas deficient in refractory elements, because they condense in grains maintained in the disc by radiation pressure, is responsible for the depletion patterns observed at the surface of numerous post-AGB systems and slows the evolution of the post-AGB star.

We estimate binary post-AGB lifetimes to range from  $2.5 \times 10^4$  yr to  $10^5$  yr which are long compared to single-star models that predict only  $10^3$  to  $10^4$  yr. Although the disc lifetime represents the major uncertainty, our model reproduces the eccentricities of most post-AGB systems on the derived lower limit of the disc lifetime. Three long-period systems show higher eccentricities than expected and require more efficient eccentricity-pumping. However, extending the disc lifetime to its expected maximum lifetime of  $10^5$  yr solves the problem. On the other hand, our model underestimates the eccentricities of long-period post-AGB stars because we assume all systems to have initially circular orbits while systems with periods longer than 2,000 d are not efficiently circularised by tides during the AGB phase. Moreover, the circumbinary disc is formed during the AGB phase so that eccentricity-pumping already operates on the AGB.

Finally, Ba, S, CH and CEMP stars experience a similar evolution than post-AGB stars and show similar period and eccentricity distributions. This suggests that interaction with a circumbinary disc is also a key mechanism in the evolution of Ba, S, CH and CEMP stars.

*Acknowledgements.* TD would like to thank Thomas Masseron, Sophie Van Eck, Philipp Podsiadlowski, Clio Gielen, Nadya Gorlova and Steve Lubow for many useful discussions. This work has been partially funded by an *Action de Recherche Concertée* from the *Direction générale de l'enseignement non obligatoire et de la*

*Recherche Scientifique – Direction de la Recherche Scientifique – Communauté Française de Belgique.*

## References

- Angeloni, R., Contini, M., Ciroi, S., & Rafanelli, P. 2007, *A&A*, 472, 497
- Artymowicz, P., Clarke, C. J., Lubow, S. H., & Pringle, J. E. 1991, *ApJ*, 370, L35
- Artymowicz, P. & Lubow, S. H. 1994, *ApJ*, 421, 651
- Blöcker, T. 1995, *A&A*, 299, 755
- Bonačić Marinović, A. A., Glebbeek, E., & Pols, O. R. 2008, *A&A*, 480, 797
- Bujarrabal, V., Castro-Carrizo, A., Alcolea, J., & Neri, R. 2005, *A&A*, 441, 1031
- Chesneau, O. 2011, in *Asymmetric Planetary Nebulae 5 Conference*
- Costero, R., Tapia, M., Méndez, R. H., et al. 1986, *Revista Mexicana de Astronomía y Astrofísica*, 13, 149
- de Ruyter, S., van Winckel, H., Maas, T., et al. 2006, *A&A*, 448, 641
- de Val-Borro, M., Karovska, M., & Sasselov, D. 2009, *ApJ*, 700, 1148
- Dermine, T., Jorissen, A., Siess, L., & Frankowski, A. 2009, *A&A*, 507, 891
- Deroo, P., Acke, B., Verhoelst, T., et al. 2007a, *A&A*, 474, L45
- Deroo, P., van Winckel, H., Verhoelst, T., et al. 2007b, *A&A*, 467, 1093
- Dullemond, C. P., Dominik, C., & Natta, A. 2001, *ApJ*, 560, 957
- Frankowski, A. & Jorissen, A. 2007, *Baltic Astronomy*, 16, 104
- Frankowski, A. & Tylenda, R. 2001, *A&A*, 367, 513
- Gänsicke, B. T., Marsh, T. R., Southworth, J., & Rebassa-Mansergas, A. 2006, 314, 1908
- Gesicki, K., Zijlstra, A. A., Szyszka, C., et al. 2010, *A&A*, 514, 54
- Gielen, C., Bouwman, J., van Winckel, H., et al. 2011, *A&A*, 533, A99
- Gielen, C., van Winckel, H., Min, M., Waters, L. B. F. M., & Lloyd Evans, T. 2008, *A&A*, 490, 725
- Gielen, C., van Winckel, H., Reyniers, M., et al. 2009, *A&A*, 508, 1391
- Gielen, C., van Winckel, H., Waters, L. B. F. M., Min, M., & Dominik, C. 2007, *A&A*, 475, 629
- Goldreich, P. & Tremaine, S. 1979, *ApJ*, 233, 857
- Hajduk, M., Zijlstra, A. A., & Gesicki, K. 2008, *A&A*, 490, L7
- Hartmann, L., Calvet, N., Gullbring, E., & D'Alessio, P. 1998, *ApJ*, 495, 385
- Hollenbach, D. J., Yorke, H. W., & Johnstone, D. 2000, *Protostars and Planets IV*, 401
- Ivezic, Z. & Elitzur, M. 1997, *MNRAS*, 287, 799
- Izzard, R. G., Dermine, T., & Church, R. P. 2010, *A&A*, 523, 10
- Jura, M., Balm, S. P., & Kahane, C. 1995, *ApJ*, 453, 721
- Kahane, C. & Jura, M. 1996, *A&A*, 310, 952
- Kashi, A. & Soker, N. 2011, *MNRAS*, 417, 1466
- Kilic, M., Kowalski, P. M., Reach, W. T., & von Hippel, T. 2009, *ApJ*, 696, 2094
- Lamers, H. J. G. L. M., Zickgraf, F.-J., de Winter, D., Houziaux, L., & Zorec, J. 1998, *A&A*, 340, 117
- Lubow, S. H. & Artymowicz, P. 1996, in *NATO ASIC Proc. 477: Evolutionary Processes in Binary Stars*, ed. R. A. M. J. Wijers, M. B. Davies, & C. A. Tout, 53
- Lubow, S. H. & Artymowicz, P. 2000, *Protostars and Planets IV*, 731
- Maas, T., Van Winckel, H., & Lloyd Evans, T. 2005, *A&A*, 429, 297
- Mastrodomos, N. & Morris, M. 1998, *ApJ*, 497, 303
- Mathieu, R. D. 1992, in *Binaries as Tracers of Star Formation*, ed. A. Duquennoy & M. Mayor, 155–169
- Mathieu, R. D. 1994, 32, 465
- Mathieu, R. D., Adams, F. C., Fuller, G. A., et al. 1995, 109, 2655
- Mathieu, R. D., Adams, F. C., & Latham, D. W. 1991, 101, 2184
- Meilland, A., Stee, P., Vannier, M., et al. 2007, *A&A*, 464, 59
- Mohamed, S. & Podsiadlowski, P. 2010, in *American Institute of Physics Conference Series*, Vol. 1314, American Institute of Physics Conference Series, ed. V. Kologera & M. van der Sluys, 51–52
- Netolický, M., Bonneau, D., Chesneau, O., et al. 2009, *A&A*, 499, 827
- Nordhaus, J. & Blackman, E. G. 2006, *MNRAS*, 370, 2004
- Podsiadlowski, P., Joss, P. C., & Hsu, J. J. L. 1992, *ApJ*, 391, 246
- Pollard, K. H. & Cottrell, P. L. 1995, in *Astronomical Society of the Pacific Conference Series*, Vol. 83, IAU Colloq. 155: *Astrophysical Applications of Stellar Pulsation*, ed. R. S. Stobie & P. A. Whitelock, 409
- Pols, O. R., Karakas, A. I., Lattanzio, J. C., & Tout, C. A. 2003, in *Symbiotic Stars Probing Stellar Evolution (ASP Conf. Proc. 303)* (San Francisco: Astronomical Society of the Pacific), 290

- Reyniers, M. & van Winckel, H. 2007, *A&A*, 463, L1
- Rödig, C., Dotti, M., Sesana, A., Cuadra, J., & Colpi, M. 2011, ArXiv e-prints
- Sandquist, E. L., Taam, R. E., Chen, X., Bodenheimer, P., & Burkert, A. 1998, *ApJ*, 500, 909
- Schuerman, D. W. 1972, 19, 351
- Sion, E. M., Holberg, J. B., Oswalt, T. D., McCook, G. P., & Wasatonic, R. 2009, *AJ*, 138, 1681
- Soker, N. 2000, *A&A*, 357, 557
- Sytov, A. Y., Bisikalo, D., Kaigorodov, P., & Boyarchuk, A. 2009, *Astronomy Reports*, 53, 223
- Theuns, T., Boffin, H. M. J., & Jorissen, A. 1996, *MNRAS*, 280, 1264
- Theuns, T. & Jorissen, A. 1993, *MNRAS*, 265, 946
- van Rensbergen, W., de Greve, J. P., Mennekens, N., Jansen, K., & de Loore, C. 2011, *A&A*, 528, A16
- Van Winckel, H. 2003, *Ann. Rev. Astron. Astrophys.*, 41, 391
- Van Winckel, H., Lloyd Evans, T., Briquet, M., et al. 2009, *A&A*, 505, 1221
- Van Winckel, H., Lloyd Evans, T., Reyniers, M., Deroo, P., & Gielen, C. 2006, *Mem. Soc. Astron. Ital.*, 77, 943
- van Winckel, H., Waelkens, C., & Waters, L. B. F. M. 2000, in *IAU Symposium*, Vol. 177, *The Carbon Star Phenomenon*, ed. R. F. Wing, 285
- Waters, L. B. F. M., Beintema, D. A., Zijlstra, A. A., et al. 1998, *A&A*, 331, L61
- Waters, L. B. F. M., Trams, N. R., & Waelkens, C. 1992, *A&A*, 262, L37
- Weidenschilling, S. J. & Jackson, A. A. 1993, *Icarus*, 104, 244
- Yasui, C., Kobayashi, N., Tokunaga, A. T., Saito, M., & Tokoku, C. 2010, *ApJ*, 723, L113
- Zahn, J.-P. 1977, *A&A*, 57, 383